Extension in Flow of a DNA Molecule Tethered at One End

Bruno H. Zimm

Department of Chemistry and Biochemistry, University of California (San Diego), 9500 Gilman Drive, La Jolla, CA 92093-0314

Received April 22, 1998; Revised Manuscript Received July 10, 1998

ABSTRACT: A theory was developed for the steady-state extension of a wormlike chain, such as DNA, in flowing liquid with one end of the molecule tethered to a fixed object. This relates to recent experiments with individually imaged DNA molecules by Perkins, Smith, Larson, and Chu. The theory is based on the familiar Oseen tensor (also called Stokeslet) formalism of chain-molecule hydrodynamics applied to a bead-segment model. With the steady-state condition a normal-mode analysis is not necessary. The calculations are carried almost to the completely stretched state at high flow rates, and reproduce the experiments well with a persistence length of 49.3 nm for the stained DNA. Measurements of extension of tethered single molecules in flow analyzed by the method described here seem to make an excellent method for determining the persistence length of individual molecules.

Introduction

Recently individual DNA molecules have been visualized, and their response to various stresses has been directly observed.[1,2] Bustamante, Marko, Siggia, and Smith,[3] analyzing measurements on individual DNA molecules by Smith, Finzi, and Bustamante,[4] demonstrated that the elasticity of DNA in stretching could be fit successfully by the well known wormlike-chain model.[5] The DNA was stretched by applying a known force to the ends of the molecule. Similar experiments have just been reported by Block and co-workers.[2] In this paper we relate to experiments by Perkins, Smith, Larson, and Chu[6] who held one end of a DNA chain fixed while the solvent was caused to flow past at a constant rate; they were then able to measure the extension of the chain as a function of flow rate. The extensions measured covered a wide range, from about 10 to 80% of the contour length.

The question arises, is the classical theory of chain-molecule hydrodynamics capable of interpreting these flow data on such a remarkable molecule and which go so far from equilibrium? In this paper we show that a method introduced by Kirkwood[7] in 1954 to calculate the diffusion coefficients of Gaussian chain molecules successfully describes the extensions of DNA, modeled as a wormlike chain, under the conditions of Perkins *et al.* With hydrodynamic interaction taken into account, we can determine the persistence length of the DNA that gives the best fit of the theory to the data; the values found, with an average of 49.3 nm, are close to those of Bustamante and co-workers.[3,4] Hydrodynamic interaction decreases with stretching, but contrary to naive expectation, it is still strong in the stretched chains.

A parallel study of the same question by Larson and co-workers[8] shows results with which we are mainly in accord. Marko and Siggia[9] had already given a preliminary treatment. Bustamante and Stigter[10] have treated the problem with a somewhat different approach but with similar results.

Model

Wormlike Chain, WLC. The molecule is modeled as a Kratky−Porod, or wormlike chain[5] (abbreviation, WLC). The WLC is characterized by two parameters, the total contour length, L, and the persistence length, P, which latter characterizes the stiffness of the chain. We assume that the contour length is fixed, which seems from previous work[2] to be a valid assumption in the force range (less than 6 pN) of the experiments of Perkins *et al.*[6] that we are analyzing. The WLC is a continuous space curve, but in order to use discrete mathematics we think of it as divided into M consecutive segments, each segment being H persistence lengths in contour, so $M = L/(HP)$, where H is an integer. See Figure 1. In contrast to the familiar random-walk model, there is no free joint between segments, flexibility residing in the segments themselves.

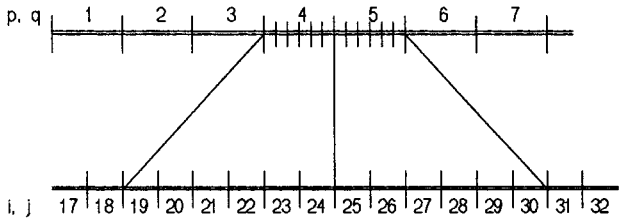

Figure 1. Division of the molecule into hydrodynamic segments indexed 1−7 (top) or into persistence-length links. The bottom diagram shows a dissection of segments 4 and 5 of the top diagram into links 19−30. For illustration in this figure the number of links per segment, H, is 6; in most of the actual calculations a value of 16 was used. The segment index p is related to the index of the link i at the left end of the segment by $i = H(p - 1) + 1$; there is a corresponding relation between q and j.

The flowing fluid exerts forces on the chain. We follow the slender-body theory of hydrodynamics[11] and imagine a continuous distribution of forces along the axis of the WLC. (The background of this methodology is discussed in Appendix A). However, for discrete computations we sample this distribution at one point in each segment. The interactions of the segments are represented by a square matrix of size M^2; handling this matrix is a severe drain on computer resources which can be controlled by selection of a suitable segment size, H. We use a value of 16 in most of this work. Fortunately, we find that H can be varied over a wide range without changing the results significantly.

S0024-9297(98)00643-3 CCC: $15.00
Published on Web 08/21/1998

Following slender-body theory we attach a "Stokeslet" to each segment. The term Stokeslet, also called the Oseen tensor, refers to a singularity in Stokes flow representing the effect of a force applied to the fluid at a point (see Appendix A). To solve the hydrodynamic problem we follow the usual procedure (Batchelor[11] and Kirkwood and Riseman[12]) of demanding self-consistency in the array of Stokeslets and attached forces representing the chain. These are the forces exerted on the chain by the flow. Once these have been found, it is straightforward to compute the deformation of the chain.

We assume that the surrounding fluid is flowing in the x direction, so that in most of what follows we can ignore the y- and z-coordinates and force components. Specifically, if the segment q experiences an x-directed drag force F_q from the flowing fluid, it contributes a component v_{pq} to the flow at segment p, where the Stokeslet equation connects the two by

$$v_{pq} = -T_{pq}F_q = -\frac{1}{8\pi\eta r_{pq}}\left(1 + \frac{x_{pq}^2}{r_{pq}^2}\right)F_q \tag{1}$$

where T_{pq} is the Oseen tensor; η is the fluid viscosity, r_{pq} is the distance between segments p and q, and x_{pq} is the x-component of this distance.

We also have the basic proportionality between the force and the local fluid velocity (Stokes' Law)

$$F_p = \rho_p v_p \tag{2}$$

where v_p is the velocity that the fluid would have at segment p if there were no segment at point p, and ρ_p is the friction coefficient of an isolated segment. The Stokes radius of the segment, which we will calculate later, is defined by

$$\rho_p = 6\pi\eta S_p \tag{3}$$

The total fluid velocity at segment p is the externally imposed velocity, V, plus the sum of all the Stokeslet contributions, eq 1

$$F_p = \rho_p(V + \sum_q v_{pq}), \quad p \neq q \tag{4}$$

which can be rewritten[12] as

$$F_p + \rho_p \sum_{q\neq p} T_{pq}F_q = \rho_p V \tag{5}$$

with T_{pq} from eq 1. If we define an Oseen matrix, h_{pq}, by

$$h_{pq} = \rho_p T_{pq} = \frac{3S_p}{4r_{pq}}\left(1 + \frac{x_{pq}^2}{r_{pq}^2}\right) \quad p \neq q \tag{6}$$

$$h_{pp} = 1 \tag{7}$$

then eq 5 converts to

$$\sum_{q=1}^{M} h_{pq}F_q = \rho_p V, \quad 1 \leq p \leq M \tag{8}$$

The explicit formula for the matrix elements h_{pq} is given in Appendix A.

Kirkwood Approximation. Equation 8 is a set of M simultaneous equations for the M unknown drag forces, F_p. It turns out that the F_p change only slowly with p. A very useful approximation due to Kirkwood[7] assumes that all the F_p are the same, equal to their average, F_{tot}/M, where F_{tot} is the total drag force on the molecule. If we substitute this in place of F_q in eq 8 we can then sum eq 8 over p and solve for F_{tot} to get

$$F_{tot} = \frac{MV\sum_p \rho_p}{\sum_p \sum_q h_{pq}} \tag{9}$$

F_{tot}/M is a good approximation to the average of the drag forces on the segments. This approximation replaces the inversion of eq 8 by a much faster summation, and at the same time avoids the singular behavior of solutions of eq 8 that can occur when some pairs of segments are too close together in space.[13] (The singularities probably are consequences of concentrating the forces on the axis of the chain when the forces are really distributed over the surface. In the literature on slender-body theory (*e.g.*, Batchelor,[11] Lighthill[14]) the bodies considered are stiff and do not have bends that bring segments into close contact, thus avoiding the problem. We look at the approximation again in Appendix D.)

Extension-Force Function of Wormlike Chain. To describe the position of the chain in space in greater detail we divide it into N "links", each link containing one persistence length of chain, so $L = NP$. The links connect $N + 1$ "beads" which are indexed by an array of N integers i running from 0 to N; bead 0 is at one end of the chain and bead N at the other. There are H links in each segment. See Figure 1.

The flowing liquid exerts a drag force, F_i, on bead indexed i, and these drag forces extend the links between the beads. No closed-form expression is known to describe the elastic properties of the WLC, but Marko and Siggia[9] have presented a useful analysis of the relation between the tension, that is, the difference between the forces on the ends, and the extension of the chain, and have derived limiting forms for low and high tension. They also have found a simple approximate formula for the tension as a function of extension, confirming Monte Carlo calculations by Vologodskii,[15] but we need the inverse of this, the extension as a function of tension. We have therefore used their variational method, which is stated to be accurate within 1.5 percent, to calculate the extension at 21 discrete values of tension, and we have used these points to generate an interpolation formula. First we follow Marko and Siggia to define a dimensionless reduced tension, f, in terms of the tension, F, in conventional units (Newtons), with P the persistence length and k_BT the thermal energy

$$f = FP/(k_BT) \tag{10}$$

The relative extension, x/l, of a piece of chain of contour length l was calculated by the variational method at values of reduced tension, f, ranging from 0.2 to 9. We interpolated the resulting points, using a least-

squares method, by a six-parameter, rational-approximation formula, $\Xi(f)$, defined by

$$\frac{x}{l} = \Xi(f) \equiv \frac{0.6667f + 0.8080f^2 + 0.10365f^3}{1 + 1.1118f + 1.1076f^2 + 0.10365f^3}, \quad f \le 9 \tag{11}$$

Two constraints were imposed before fitting to get the theoretically correct initial slope, $^2/_3$, and the correct unity asymptote; the four free parameters were then adjusted to give the best mean-squares fit. The rms deviation of $\Xi(f)$ from the points is 0.001. At values of f above 9 we adopt the asymptotic expression derived by Marko and Siggia[9]

$$\Xi(f) = 1 - 1/(4f)^{1/2}, \quad f > 9 \tag{12}$$

These two approximations join at $f = 9$ without a significant discontinuity.

Note that the relative extension, x/l, of a segment of a long WLC depends only on the reduced tension, f, and is independent of the contour length, l, of that segment,[16] regardless of whether l is greater or less than the persistence length P. (This rule does not apply to isolated short pieces of WLC.) It is important to remember that x is the average extension from the average force-free position, an extension that is due to the tension; there is also a fluctuating extension due to Brownian motion. When necessary we distinguish the two by subscripts, x_f for the former and $\langle x_0^2 \rangle$ for the latter, noting that the fluctuating extension is described by its mean square, its mean being zero. We assume that eq 11 applies to x_f even when x_f is much smaller than $\langle x_0^2 \rangle^{1/2}$; in other words, the tension-induced extension is not correlated with the Brownian (mean-square) extension.

To compare with the data, we need to calculate the mean extensions of the links and the mean positions of the beads, using a method similar to that of Perkins *et al.* Bead 0 is fixed to the origin at $x_0 = 0$, while the other beads float freely in the flow. Link i connects beads $i - 1$ and i. The tension in link i is the sum of the drag forces, f_k, on bead i and all the beads downstream from it. Let its average extension be Δ_i; then by putting $l = P$ in eq 11, we get

$$\Delta_i = P\Xi\left(\sum_{k=i}^{N} f_k\right) \tag{13}$$

Bead 0 is anchored at $x_0 = 0$, bead 1 is at $x_1 = \Delta_1$, bead 2 is at $x_1 + \Delta_2$, and so on. In general, the position of bead i is

$$x_i = \sum_{j=1}^{i} \Delta_j = P\sum_{j=1}^{i} \Xi\left(\sum_{k=j}^{N} f_k\right) \tag{14}$$

We are most interested in the position of the Nth bead, x_N, which is the maximum extension of the chain; from eq 14 we get

$$\frac{x_N}{L} = \frac{1}{N}\sum_{j=1}^{N} \Xi\left(\sum_{k=j}^{N} f_k\right) \tag{15}$$

where $L = NP$ is the contour length of the whole chain.

In the Kirkwood approximation all the forces f_k on the N beads 1 through N are the same, F_{tot}/N, so from eq 10, the f_k are

$$f_k = (P/k_B T)(F_{tot}/N) \tag{16}$$

In the counting we have omitted bead 0 since it is tethered to the substrate.

In the above we have ignored possible correlations in structure between successive links.

Friction Coefficient of a Segment, ρ_p. To proceed we need the friction coefficient of the segment, ρ_p, in eq 2. It is convenient to express this in terms of its Stokes radius as defined in eq 3, $S_p = \rho_p/(6\pi\eta)$, and to evaluate this by use of the Kirkwood approximation. We already have most of the necessary mathematical machinery in eqs 2−9, which we can generalize by thinking of them as equations applying to any slender body that can be divided into smaller parts. In this case the slender body is what we have been calling a segment, and it is divided into H links each consisting of one persistence length, P, of chain. The links are indexed by integers i and j running from $H(p - 1) + 1$ to Hp, as seen in Figure 1. Rewriting eq 9 in these terms, we find that the total drag force F_p on segment p is

$$F_p = \frac{H^2 V \rho_l}{\sum_i \sum_j h_{ij}} \tag{17}$$

where ρ_l is the friction coefficient of one link, $S_l = \rho_l/(6\pi\eta)$ is the Stokes radius of one link, and h_{ij} is given by eq A-12 of Appendix A. But by definition the friction coefficient of the segment p is $\rho_p = F_p/V$, so we get

$$S_p = \frac{H^2 S_l}{\sum_i \sum_j h_{ij}} \tag{18}$$

This quantity depends on the segment index, p, because the link positions, x_i and x_j, that are in h_{ij} depend on p.

Equation 18 is a generally applicable formula that relates the Stokes radius of a slender body to the Stokes radii of its parts and to the interactions, h_{ij}, between them. We can use it to calculate the Stokes radius of a link, but there is a simpler alternative. Each link consists of one persistence length of chain, which is rather stiff and not likely to be strongly curved; thus S_l is nearly the same for all links. We assume that the link can be approximated for hydrodynamic purposes as a randomly oriented prolate ellipsoid with major axis P and minor axis 2.5 nm, the approximate diameter of the Watson−Crick helix. Perrin's formula for the Stokes radius[17] is, with β the axial ratio

$$S_l = \frac{P(1 - \beta^{-2})^{1/2}}{2\ln[\beta(1 + (1 - \beta^{-2})^{1/2})]} \tag{19}$$

If we take P to be 50 nm (anticipating results described below) so β is 20, we obtain the Stokes radius of one bead-link, $S_l = 0.1354P$; the coefficient 0.1354 is almost independent of the assumed axial ratio because the logarithm is a slowly varying function. We have also confirmed this value by the Kirkwood method, taking the link to be a pearl necklace of 20 2.5 nm spheres, and found the results for S_l were practically the same as eq 19. We use eq 19 in what follows.

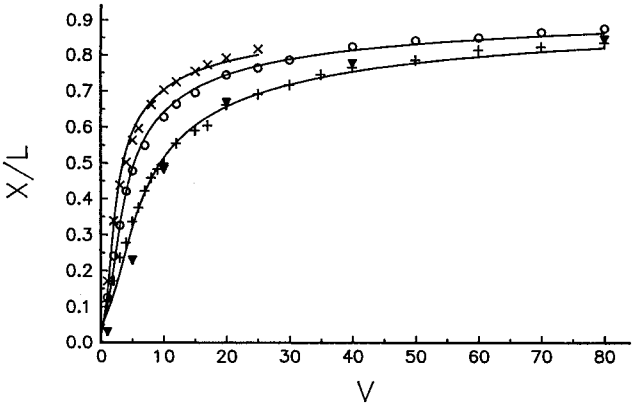

Figure 2. Relative extension, the x-position of the edge of the density distribution, eq C-8, divided by the contour length, as a function of flow velocity, V, in μm/s. Symbols, except for the triangles, are the experimental points from a private communication by Thomas Perkins, who used the procedures described in Perkins *et al.*;[6] curves are cubic spline interpolations of our theoretical calculations done at the experimental values of V. The lowest curve is the 44 μm molecule; the middle curve is the 89.5 μm molecule; the top curve is the 151 μm molecule. The black triangles show the approximate theory of Marko and Siggia;[20] see the main text.

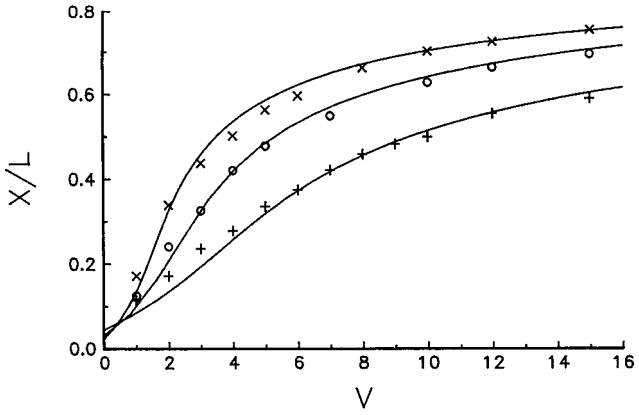

Figure 3. Left part of Figure 2 enlarged.

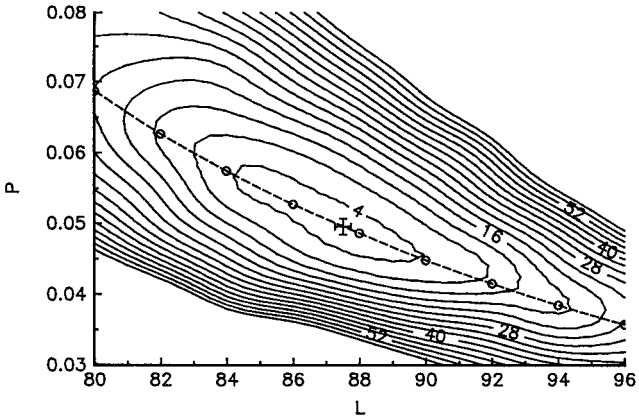

Figure 4. Contour plot of the figure-of-merit surface above the L,P plane of the 89.5 μm molecule. The numbers on the contours are 10^4 times the figure of merit. The dashed line marks the valley floor; the cross marks the global minimum. Axis scales are μm.

Iterating for Self-Consistency. We now have developed all the machinery needed to compare theory with the experimental data on chain extension as a function of fluid velocity, with persistence length and contour length being the only adjustable parameters. For data we used three molecules of nominal contour length 44, 89.5, and 151 nm from the paper by Larson *et al.*;[8] these were selected in consultation with T. Perkins as representing the best data.

Since bead positions depend on drag forces and drag forces depend on bead positions, both with nonlinear relations, we have to proceed by repeated trials and adjustments until we get values that are consistent with each other. We set up the following algorithm for each value of V:

1. Assume a trial value for the persistence length, P. Select a value of V and carry out the following steps 2 through 5.

2. Assume a trial value for the force, F_{tot}.

3. Use this trial value in the WLC force law, eqs 11 and 12, to get the bead positions, x_i, by eq 14, and from them the link and then the segment positions, x_p. Recall that one segment contains $H = 16$ links; see Figure 1.

4. Use these x_p in the h_{pq} matrix to compute a new value of F_{tot} by eq 9.

5. Introduce this new value of F_{tot} as the trial value in step 2, and iterate steps 2 through 5 until the computed value of F_{tot} is the same as the last trial value. Typically about 15 iterations reduce the relative difference to 10^{-7} or less.

For the selected value of velocity, V, this process converges on a drag force, F_{tot}, and a set of bead positions, x_i, that are consistent with each other. From the position, x_N, of the last segment we get the relative extension, x_N/L. By repeating this calculation for all the measured values of V, we get values of the relative extension as a function of V which can be compared to the experimental data of Perkins *et al.* on the same quantities.

(A small term has to be added to x_N to take account of the effect of fluctuations on the image of the molecule and on the experimental process of extracting the value of x_N from this image. This is explained in Appendix C.)

We then attempt to find the value of P that gives the best fit to all the data on a particular molecule by repeating steps 1−5, adjusting the persistence length, P, to minimize an appropriate "figure of merit". We take the figure of merit to be the sum, divided by the number of data points, of the squares of the differences between the calculated and the experimental data of x_N/L for the whole set of V values of this molecule. Minimizing this figure of merit is thus done by fitting to the data by a least-squares procedure. About 10 iterations with different values of P locate the best-fit value of P within a few tenths of one percent. For examples of the curves thus generated, see Figures 2 and 3.

Another parameter that enters the calculation is the contour length, L. At first we used the values estimated by the experimenters, but we soon found that we could improve the fit to the data by adjusting this length. For example, consider the case of the so-called 89 molecule initially thought to be 89.5 μm long. Accepting this value of the length leads to a best-fit value for P of 45.49 nm with a figure of merit of 2.99×10^{-4}. However, varying the length as well as P leads to a best-fit P of 49.51 nm and a best-fit length of 87.51 μm, with the figure of merit improved to 1.91×10^{-4}. Figures 4 and 5 show a contour plot on the L, P plane of the part of the figure-of-merit surface near its minimum, which is marked by the cross. The dashed line shows the lowest

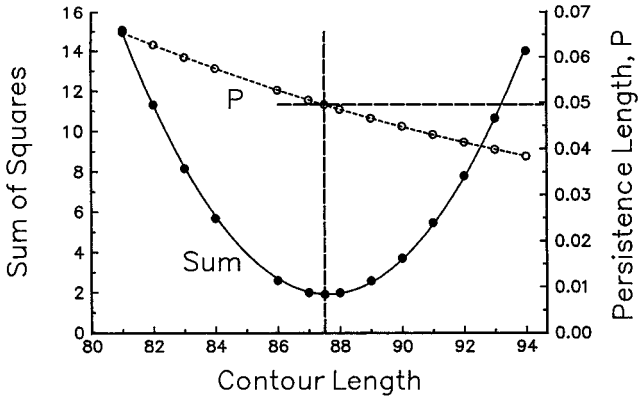

Figure 5. Plot of 10^4 times the figure of merit (left vertical axis) along the floor of the valley in the surface of Figure 4 (dashed line in Figure 4.) The values of P (right y-axis) along the line are also shown. The values of L and P at the figure-of-merit minimum are marked by the crossing straight lines. Horizontal and right vertical axis scales are μm.

Table 1. Best-Fit Contour and Persistence Lengths

nominal length, μm	best-fit length, μm	persistence length, nm	figure of merit
44	43.18	50.63	2.817×10^{-4}
89.5	87.51	49.51	1.910×10^{-4}
151	145.04	48.18	3.411×10^{-4}

path on this surface, that is, the floor of the valley. Figure 5 shows a plot of the figure of merit along this lowest path and the values of P on this path. It is obvious that the minimum is well-defined.

The process is thus an iterative search in three dimensions, first varying F_{tot} to find consistency with the bead positions, then varying L and P to find the values that give the best figure of merit for a particular molecule.[18] In the end we have succeeded in finding the persistence length and contour length that best fit the data on this molecule.

Results and Discussion

The results on the three molecules of Larson *et al.* are shown in Table 1. The persistence lengths are in reasonable agreement with values, 45−50 nm, determined by older methods[19] and with the 53 nm of Bustamante and co-workers[3] from tethered DNA stretched by a magnetic bead at the free end.

Figures 2 and 3 show the calculated extension curves for the three DNA molecules together with the experimental data. Since all molecules had the same composition, being concatenmers of λ-phage DNA (Perkins et al.[3]), we used the average persistence length, 49.44 nm, in calculating all three of these curves, but each with its best-fit contour length. The calculated curves follow the data closely with a root-mean-square deviation (the square root of the average figure of merit of all three curves) of 1.7% in x/L. We emphasize that same value of the persistence length was used to produce all three curves; the mean figure of merit was 2.872×10^{-4}. Thus all three molecules appear to have the same elastic properties, as expected.

The deviations of the experimental points from the calculated curves in Figure 3 seem to be essentially random, which suggests that these deviations are caused by random measurement errors. The measurements become more difficult at low flow rates where the molecular extensions are small and the fluctuations relatively larger.

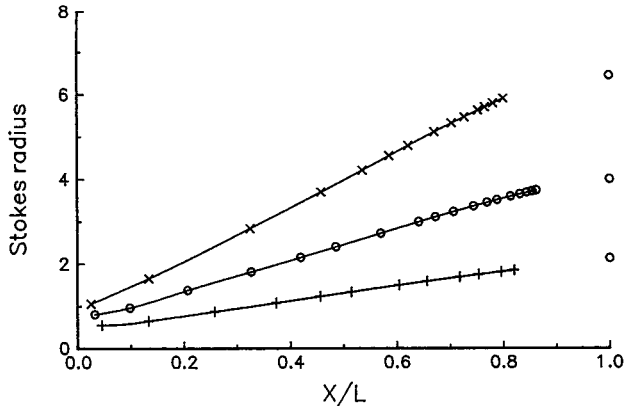

Figure 6. Stokes radii in μm of the three whole molecules plotted against the relative extension. The three curves from top to bottom represent the 151, 89.5, and 44 μm molecules, respectively. The symbols are the radii calculated at the various observed values of V, and the curves are cubic-spline interpolations of these points. The lone circles at the right are the Stokes radii of prolate ellipsoids, eq 18, with the same axial ratios as the DNA molecules.

The crossing of the extension curves near $V = {}^1/_2$ in Figure 3 denotes the boundary between two regimes; at low flows the extension, x_N, scales as $L^{1/2}$ because the chain is a random walk (see Appendix B), but at high flows the chain responds approximately linearly to the drag force which scales approximately as $L \ln(L/P)$. This thought has been elaborated on by Marko and Siggia,[20] and they proposed an approximate theory for the extension as a function of V. The black triangles in Figure 2 were calculated numerically from their eqs 7, 25, and 27; the agreement is clearly quite good except at the lowest flow rates. We made no attempt to find the best values of the parameters in their formula, so improvement is probably still possible.

It is also of interest to see how the drag force, F_{tot}, depends on the flow rate and the accompanying extension. This is conveniently expressed by the Stokes radius, S_{wm}, of the whole molecule, the parameter in Stokes' law

$$S_{wm} = \frac{F_{tot}}{6\pi\eta V} \tag{20}$$

Figure 6 shows the results. The radius rises in a simple, almost linear, curve as extension increases, and the interior of the chain becomes more exposed to the flow. There is no sign of an abrupt "coil-stretch" transition. Moreover, the molecule never becomes so exposed as to be properly called free-draining. The closest approach to free draining in our results is the 44-molecule in a flow of 80 μm/s, where the Stokes radius is 1.847 μm, while the free-draining radius, calculated as $\sum_p S_p$, would be 3.336 μm. (Here S_p was calculated from eq 18.) Even though the molecule is extended to 82% of its contour length, its Stokes radius is barely more than half of the free-draining value.

The total force on the molecule, F_{tot}, is given by $6\pi\eta S_{wm}$; for example, the force on the 89.5-molecule, using $\eta = 0.95$ m (Pa s), $V = 80$ μm/s, and $S_{wm} = 3.7429$ μm is 5.36 pN. This is the largest value encountered in this study.

Comparison to Other Work. Larson, Perkins, Smith, and Chu[8] analyze the same set of data. Their model is similar, but they use Monte Carlo instead of analytical methods, and have a different way of getting

the Stokes radius of a segment. They present an interesting comparison to a simple dumbbell model. They also get a quantitative fit to the data, using a value of 53 nm for P; no attempt was made to find a best value for P. (Doing our calculation with $P = 53$ and $L = 89$ yields a figure of merit of 9.567×10^{-4}, worse than our best-fit value of 1.910×10^{-4}, but still close to the experimental precision.) Using D. Smith's measured DNA diffusion coefficients,[21] they are able to avoid the excluded-volume problem and get a scaling exponent, which apparently is not constant, rising from 0.54 to 0.75 as the contour length is increased. Concerning the exponent, see Appendix C.

Bustamante and Stigter[10] also analyze the same set of data with a model similar to ours, though differing in a number of important details. They get an acceptable fit to the data using a value of 67.5 μm for P. Because of the many differences between the two calculations, we have not attempted to hunt down the cause of the discrepancy in the persistence lengths. These authors also make an interesting application of the theory to the extension of tethered DNA in steady state electrophoresis.

Long, Viovy, and Ajdari[22] and Bustamante and Stigter[10] have shown that the stretching of tethered DNA in flow is closely related to the stretching of the same molecule in an electric field, the flow velocity being replaced by the electrophoretic mobility of the free molecule. Long et al. have also discussed the problem of the scaling exponent.

Miscellaneous

A number of minor approximations have been made in these calculations. We have used only the random-orientation value of the segment Stokes radius; introducing the true orientation dependence of each segment could be done but would slow the calculation significantly and would have only minor effect on the results. We have ignored the known stretching of the contour length under stress[2,23,24] which becomes significant at stresses greater than about 10 pN; the highest stress reached in this study is 5.36 pN in the 89.5 molecule at $V = 80$ μm/s as calculated from the Stokes radii of Figure 6 by eqs 2 and 3. The dramatic structural phase transition[23,24] (not a coil−stretch transition) that appears at stresses around 70 pN is likewise not involved in our calculations. Excluded volume effects have been neglected; these would presumably be most important at low flow rates where relatively large experimental errors make analysis tenuous. It seems unlikely that such effects would be significant when the molecule is extended to a substantial fraction of its contour length. (See also discussion by Marko and Siggia.[9]) Replacing the Kirkwood approximation by solving the simultaneous equations, eq 8, is feasible but of uncertain value because of the danger of the singularities found by Zwanzig et al.,[13] singularities that these authors showed can even make the Stokes radius become negative. However, we find in Appendix D that solving the equations does not seem to lead to such catastrophic results in our problem; this method invites further study.

The reproducibility of the persistence length is shown by the agreement of the three independent determinations on molecules differing by more than a factor of three in contour length, the three values lying within 2.5% of the mean. Since all three molecules examined had the same composition, the possibility that the persistence length depends on the base-pair sequence does not come into the comparison of the three, likewise the possibility that these molecules contain intrinsic bends. On other hand, the absolute accuracy of these values is hard to estimate, involving as it does both experimental and theoretical problems. It is important to remember that the λ-DNA used by Perkins and co-workers was not strictly native; it was stained by a fluorescent dye and was in a solution in which the concentration of positive ions (approximately 10 mM) was uncertain because of partial ionization of the Tris and EDTA buffer. Though the apparent agreement of the results with those of Bustamante and co-workers[4] is gratifying, it is not as meaningful as one would like because the conditions were somewhat different.

Conclusion

In answer to the question raised at the beginning, we can say that the theory of the wormlike chain combined with Kirkwood's approximation for the hydrodynamics quantitatively describes the stretching of an individual DNA molecule by flowing liquid. In the process we obtain a respectably precise value for the persistence length of that molecule. The calculations were easily done on a modest (50 MHz) personal computer. This and related methods applied to experiments on single DNA molecules look very attractive for getting precise values of the persistence lengths of molecules with particular base-pair sequences.

Acknowledgment. I am indebted to Dr. Thomas T. Perkins for discussions that led to this work and for providing copies of the data. I am indebted to Ron Larson for preprints of ref 8. Extensive correspondence with Dirk Stigter has been most valuable. A grant from the Wyatt Technology Corp. provided financial support.

Appendix A. The Oseen Tensor and the Stokeslet

Background. The theory of hydrodynamic interactions in macromolecules that goes by the above names has had a curious history. An early use was by J. M. Burgers[25] in 1938 who considered the hydrodynamics of long thin rods by seeking self-consistency of the forces on the rods and the flows produced by these forces. He approximated the forces on the rod surface by forces on the axis of the rod, and introduced the notion that a force $\mathbf{F}_p$ exerted on the fluid of viscosity η at point p would generate a flow at another point q with velocity $\mathbf{v}_{pq}$ given by

$$\mathbf{v}_{pq} = \frac{1}{8\pi\eta r_{pq}}(\mathbf{1} + \mathbf{r_{pq}}\mathbf{r_{pq}}) \qquad \text{(A-1)}$$

(Here bold-faced type indicates a vector, and the unity in the last term is a dyadic.) In the special case that the force is directed along the x-axis and we need only the x-component of $\mathbf{v}$, this formula reduces to eq 1 of the main text. Burgers derived this formula from a much more complicated general formula given by Oseen,[26] and he referred to it as the Oseen tensor. It is essentially a Green's function of the linearized Navier−Stokes differential equations. Hermans,[27] Kirkwood and Riseman,[12] Kirkwood,[7] and Zimm[28] applied the Oseen tensor formalism to the random-coil model of a macromolecule.

Also starting from Burgers' work, and apparently independent of the publications just cited, was the development of "slender-body theory". G. J. Hancock[29] in 1953 in a paper on "The Self Propulsion of Microscopic Organisms Through Liquids" introduced "a singularity peculiar to viscous motion, which will here (for want of a better word) be called a 'Stokeslet'." This singular flow was in fact just the Oseen tensor. Later Batchelor[11] in a much quoted paper applied the term slender-body theory to the Burgers method, stating "the basic idea of slender-body theory is the replacement of the body by a line of Stokeslets." A considerable literature has developed on this subject, most dealing with bodies that are either straight or smoothly curved; see Lighthill,[14] for example.

Matrix Elements. The Oseen matrix elements h_{pq} of eq 8, which describe the interactions between the hydrodynamic segments, have to be put in a form suitable for a wide range of flow velocities and molecular conformations. We consider first the case where the fluid velocity, V, is small and the molecule is only slightly perturbed fron its random-coil equilibrium state. In this case the distribution of segments is approximately isotropic, and we can average first over all directions of r_{pq}; the average of x_{pq}^2/r_{pq}^2 equals 1/3. From eq 6 of the main text

$$\langle h_{pq}\rangle = S_p\langle 1/r_{pq}\rangle, \quad p \neq q \tag{A-2}$$

Under these conditions the WLC has the familiar random-flights (Gaussian) probability distribution[5] for r_{pq}

$$\left(\frac{3}{4\pi H|p-q|P^2}\right)^{3/2} \exp\left(-\frac{3r_{pq}^{\,2}}{4H|p-q|P^2}\right) \tag{A-3}$$

$H|p-q|$ being the number of persistence lengths in the contour between segments p and q. We average over this distribution to get

$$\langle 1/r_{pq}\rangle = (3/(\pi H|p-q|))^{1/2} \tag{A-4}$$

where we have omitted explicitly writing P because we are expressing all lengths, including S_p, in units of P. Putting eq A-4 into eq A-2, we get

$$h_{pq,0} = S_p(3/(\pi H|p-q|))^{1/2}, \quad p \neq q \tag{A-5}$$

where the subscript 0 indicates the slow-flow condition. This is the classical random-coil case first considered by Kirkwood and Riseman.[12] In the averaging over the random-coil distribution, the divergence as p approaches q has been made harmless.

In most of what follows the distortion of the intersegment distances caused by the flow is much larger than the average random-walk distances, so we need to find a formula that encompasses both situations. We have already calculated in eq 14 the x-components of the mean bead positions, x_i, induced by the flow. As shown in Figure 1, we locate the position of hydrodynamic segment p at that of bead i where the indices p and i are related by

$$i = H(p-1) + 1 \tag{A-6}$$

We can thus get x_p from x_i and then calculate the x-components of the intersegment distances

$$x_{pq} = x_p - x_q$$

We shall assume that the y and z components of the intersegment distance r_{pq} are small in comparison to the x component except when the tension between the segments p and q is very weak, and in that case we already have eq A-5 from the random-coil distribution. On the other hand when the tension between segments p and q is strong, x_{pq} is much larger than y_{pq} and z_{pq}, so the difference between r_{pq} and x_{pq} is second-order small. To take advantage of this, we define $\langle x_{pq,0}^2\rangle$ as the limiting low-tension value of x_{pq}^2, and, with the low-tension values of $\langle y_{pq,0}^2\rangle$ and $\langle z_{pq,0}^2\rangle$, we get the low-tension $\langle r_{pq,0}^2\rangle = \langle x_{pq,0}^2\rangle + \langle y_{pq,0}^2\rangle + \langle z_{pq,0}^2\rangle$, and insert this in eq 6 of the main text to get

$$h_{pq} = \frac{3S_p(2\langle x_{pq,0}^{\,2}\rangle + \langle y_{pq,0}^{\,2}\rangle + \langle z_{pq,0}^{\,2}\rangle)}{4(\langle x_{pq,0}^{\,2}\rangle + \langle y_{pq,0}^{\,2}\rangle + \langle z_{pq,0}^{\,2}\rangle)^{3/2}} \tag{A-7}$$

When the tension is vanishingly weak $\langle x_{pq,0}^2\rangle = \langle y_{pq,0}^2\rangle = \langle z_{pq,0}^2\rangle$, and eq A-7 reduces to

$$h_{pq,0} = \frac{S_p}{3^{1/2}\langle x_{pq,0}^{\,2}\rangle^{1/2}} \tag{A-8}$$

We equate this to eq A-5 and solve for $\langle x_{pq,0}^2\rangle$ with the result

$$\langle x_{pq,0}^{\,2}\rangle^{1/2} = (2\pi H|p-q|)^{1/2}/3 \tag{A-9}$$

This then is the value of x_{pq} that makes eq 6 equal the low-tension form, eq A-5. To generalize to include high tension, we denote by $x_{pq,\mathrm{f}}$ that part of the extension induced by the flow as given by eq 14, and we assume that there is no correlation between $x_{pq,0}$, which is induced by Brownian motion, and $x_{pq,\mathrm{f}}$, which is induced by the flow, so that their squares add without cross-terms to make the square of the total extension, $\langle x_{pq}^2\rangle$

$$\langle x_{pq}^{\,2}\rangle = \langle x_{pq,0}^{\,2}\rangle + x_{pq,\mathrm{f}}^{\,2} \tag{A-10}$$

Assuming that the transverse fluctuations, y_{pq} and z_{pq}, are approximately independent of the tension, we put x_{pq} from eq A-10 in place of $x_{pq,0}$ in eq A-7 and get, after simplifying

$$h_{pq} = \frac{3^{1/2}S_p(9x_{pq,\mathrm{f}}^{\,2} + 2\pi H|p-q|)}{2(3x_{pq,\mathrm{f}}^{\,2} + \pi H|p-q|)^{3/2}} \tag{A-11}$$

This is the segment-interaction function. Equation 18 of the main text for the Stokes radius of one segment needs the corresponding expression, h_{ij}, for the interaction between a pair of links. This is easily obtained by setting H to unity and replacing p and q by i and j respectively, in accord with eq A-6, and replacing S_p by S_l. The result is

$$hij = \frac{3^{1/2}S_l(9x_{ij,\mathrm{f}}^{\,2} + 2\pi|i-j|)}{2(3x_{ij,\mathrm{f}}^{\,2} + \pi|i-j|)^{3/2}} \tag{A-12}$$

These formulas are well behaved as $x_{pq,\mathrm{f}}$ or $x_{ij,\mathrm{f}}$ approach zero. Figure 7 shows how they reduce to eq

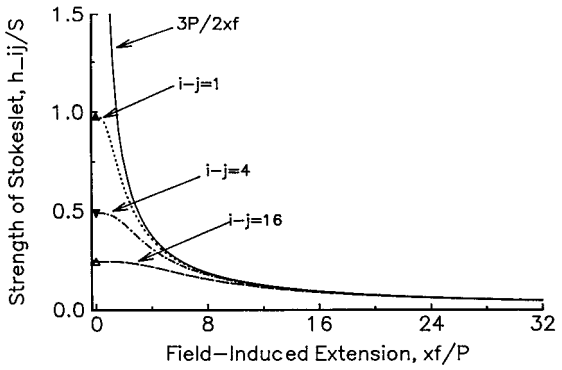

Figure 7. Hydrodynamic-interaction function h_{ij}/S_I (Stokeslet or Oseen tensor) between a pair of links i,j, as a function of the field-induced extension, $x_{ij,f}$ of the interlink distance, r_{ij}. The solid curve is the asymptotic form, eq 5, with $x_{ij} = r_{ij}$. Dashed curves are eq A-12 with three different values of $i - j$. Triangles are the values of the Kirkwood−Riseman expression for the random coil, eq A-5. Equation 5 becomes singular at the origin, while eq A-12 approaches the random-coil expression and remains well behaved. Equation A-11, the interaction between a pair p,q of hydrodynamic segments, is exactly the same function with the parameter $|i - j|$ replaced by $H(|p - q|)$; both parameters are the number of persistence-length links between the members of the interacting pair.

A-5 as the force-produced extension goes to zero and reduce to eq 6 of the main text as the force approaches infinity and $x_{pq,f}$ approaches r_{pq}, and approximate the average of eq 1 over the whole range of tensions; they are what we use in our calculations. They could be criticized because of the assumption that the average transverse fluctuation is independent of tension when actually it decreases at high tension, but a correction would be second order and small. We also included a small correction to h_{pq}, using an image-force method, to account for the weak effects of the walls of the chamber.

Appendix B: Exponent 0.5 in Weak Flow

We consider the case where the fluid velocity, V, is small and the molecule is only slightly perturbed from its random-coil equilibrium state. In this case eq A-5 is appropriate. We see that the matrix of h_{pq} is a "Toeplitz matrix" (all elements along any one diagonal are the same), and the double sum can be reduced to a single sum over the diagonals. This in turn can be converted to an integral by the Euler−MacLaurin formula. The result, neglecting terms of order unity relative to N, is

$$F_{tot} = (3\pi)^{3/2} N^{1/2} \eta P V/4 \qquad \text{(B-1)}$$

In the Kirkwood approximation all F_p are equal to F_{tot}/N; using this in eq 15, and taking the linear low-force limit of eq 11, we find that the relative extension, x_N/L, varies approximately as $N^{1/2}V$, which is proportional to $L^{1/2}V$, in rough agreement with the experiments of Perkins *et al*. This is to be expected only where the extension is small enough for the Gaussian approximation of eq A-3 and the linear limit of eq 11 to be valid.

It is also possible to introduce a general exponent, α, empirically reflecting non-Markovian chain statistics resulting from excluded-volume effects, in place of the random-walk exponent $^1/_2$ in eq A-4; the result is that x_N/L scales as $N^{\alpha}V$, allowing better agreement with Perkins *et al*., who prefer values from 0.54 to 0.75 as the exponent, depending on the range of molecular lengths studied.

Equation B-1 is a low-tension, low-stretch approximation not expected to hold at high flow rates. Changing the exponent in eq B-1 to 0.6 has an almost imperceptible effect on the curves (results not shown). Further, the WLC approaches a straight rod at high flow rates, and the known scaling of drag force as $L/\ln(L)$ for a straight rod of length L implies that scaling of drag with a fractional power of length for the WLC can at best be only a rough approximation valid over a limited range. Therefore the observed exponents from 0.54 to 0.75 are probably without scaling-theory significance.

Appendix C: Fluctuations and the Image of the Molecule

The experimentally observed image is not a collection of points; it is a smooth object made up of overlapping fluctuations of chain density. Consider bead i; by eq 14 and the method described in the main text we determine its mean position, x_i; we now wish to describe its fluctuations, δx_i, around this mean position. The distribution of positions will be given by a Boltzmann expression

$$\psi_i(\delta x_i) = K \exp(-U(\delta x_i)/k_B T) \qquad \text{(C-1)}$$

where $U(\delta x_i)$ is the free energy, k_B the Boltzmann constant, T the temperature, and K a normalization constant. The force on bead i is $F = -\mathrm{d}U/\mathrm{d}x_i$, and since the force is zero at the mean position of x_i, the free energy, U has a minimum there. Hence the Taylor expansion of U in terms of δx_i has no linear term; with this Taylor expansion eq C-1 becomes

$$\psi_i(\delta x_i) = K \exp\left(-\frac{\mathrm{d}^2U/\mathrm{d}x_i^2 \delta x_i^2}{2k_B T}\right) = K \exp\left(\frac{\mathrm{d}F/\mathrm{d}x_i \delta x_i^2}{2k_B T}\right) \qquad \text{(C-2)}$$

where $\mathrm{d}^2U/\mathrm{d}x_i^2 = -\mathrm{d}F/\mathrm{d}x_i$ is to be evaluated at the mean position of x_i. From this, we compute the standard deviation, σ_i of δx_i

$$\sigma_i^2 = \langle \delta x_i^2 \rangle - \langle \delta x_i \rangle^2 = k_B T/(-\mathrm{d}F/\mathrm{d}x_i)_{xi} \qquad \text{(C-3)}$$

The force is the sum of two components, the drag force, F_{tot}/N, and the elastic force, F_i, from the stretched segments. Noting that F_{tot} is a function of all the interbead distances of the whole chain, we assume that the fluctuations of the rest of the chain are only weakly correlated with those of bead i, so F_{tot} is constant as bead i fluctuates and F_{tot} does not contribute to $(\mathrm{d}F/\mathrm{d}x)_{xi}$. For the elastic force we use Marko and Siggia's approximate WLC interpolation formula (with a negative sign because the force is antiparallel to the extension):

$$F_i = -\frac{k_B T}{P}\left(\frac{1}{4(1 - x_i/(iP))^2} - \frac{1}{4} + \frac{x_i}{iP}\right) \qquad \text{(C-4)}$$

(This is approximately the inverse of eqs 9 and 10.) Introducing it into eq C-3, we get

$$\sigma_i = \left(\frac{2iP^2}{2 + (1 - x/(iP))^{-3}}\right)^{1/2} \qquad \text{(C-5)}$$

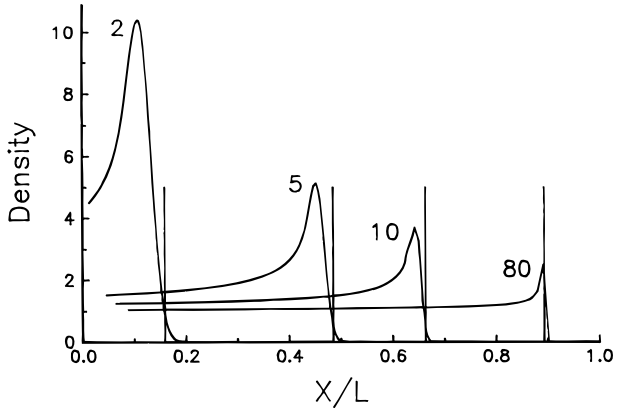

Figure 8. Total segment density of the 89.5 μm molecule as a function of x/L at four values of the flow velocity V. The numbers above the curves are the corresponding flow velocities in μm/s. For this example the molecule was divided into 75 hydrodynamic segments of length 1.1933 μm, each containing nine links. The vertical scale has units that are arbitrary but are the same for all four curves. The vertical lines are the visually estimated apparent edges of the density distribution, eq C-8.

The total bead density, $\Psi(x)$, is the sum of all the individual densities. We designate the actual position of the ith bead as $w_i = x_i + \delta x_i$. The probability distribution of w_i, $\omega_i(w_i)$, is obtained from that of the corresponding δx_i. Thus from eqs C2, C3, and C5

$$\omega_i(w_i) = \psi_i(w_i - x_i) = (2\pi\sigma_i^2)^{-1/2} \exp(-(w_i - x_i)^2/(2\sigma_i^2)) \quad \text{(C-6)}$$

Then the total density of beads at position x is the sum over the ω_i with all w_i equal to x:

$$\Psi(x) = \sum_{i=1}^{N} \omega_i(x) = \sum_{i=1}^{N} \psi(x - x_i) \quad \text{(C-7)}$$

To avoid artifactual oscillations arising from the discrete bead-link model, we smooth the density by setting σ_i to P whenever eq C-5 yields a smaller value; this redistributes density from a bead position to its adjacent links without changing the average density. In Figure 8, as an example, we show plots of the segment density, eq C-7, for a chain with contour length 89.5 μm for four different values of the fluid velocity V. The curves show a characteristic peak as they approach full extension. This peak comes about because the forces on the high-index beads are small (compare with eq 13), so these beads remain close to each other, and, with their fluctuations overlapping, appear as a cluster. The peak appears also in the experiments by Perkins *et al.*

We also have to consider the effect of fluctuations on the experimental measurement of chain extension. Perkins *et al.* measured the length of images of the fluorescently stained molecule. They had to make a subjective judgment of where the downstream edge of the image was. The distribution of the bead N is a Gaussian, eq C-6; we estimate that the perceived edge of this distribution comes where the density is one fourth of the density at the peak; this is at

$$x_N + (2 \ln(4))^{1/2}\sigma_N \quad \text{(C-8)}$$

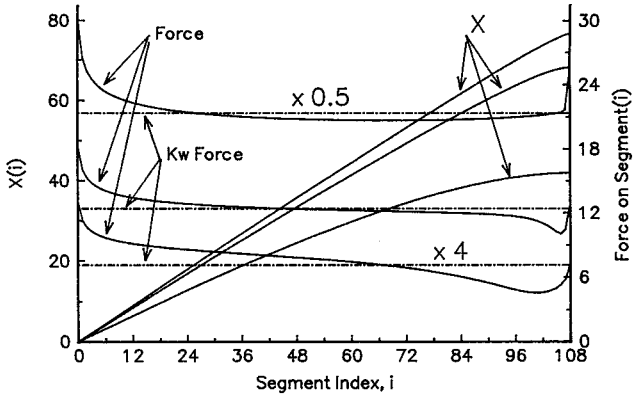

Figure 9. Investigating the Kirkwood approximation using the 89.5 μm molecule as an example. Forces on segments and positions of segments of the 89.5-molecule: upper curves in 80 μm/s flow; middle curves in 25 μm/s flow; lower curves in 5 μm/s flow. Left y-axis goes with the positions of the segments (curves marked "X") in μm; right y-axis with the forces on the segments in fN. Positions were first calculated by the Kirkwood approximation (curves marked "X"); then, with these positions used to make the h_{pq}, the forces from the full solution of eq 8 were calculated; these are the solid curves marked "Force". The Kirkwood approximation forces are the dot−dash curves. To show all curves on the same graph, the 80 μm/s forces have been multiplied by 0.5 and the 5 μm/s forces have been multiplied by 4. The molecule was modeled as 109 segments of 16 persistence lengths each; segment 0 was anchored to $x = 0$, and segment 108 was the free end. The segment friction coefficients, ρ_p, on the right-hand sides of the equations were calculated from eqs 3 and 18 using a value of 0.95 m(Pas) for η. The h_{pq} of eq A-11 were used with $x_{pq,f}$ intersegment distances calculated as described in step 5 of the iteration algorithm. H was set to 16.

This position is indicated by the vertical line on each of the curves in Figure 8.

Appendix D: The Kirkwood Approximation Compared to Full Solution

To examine the Kirkwood approximation, we solved the set of equations, eq 8, for the forces using the 89.5 molecule as an example. Figure 9 shows the results for three values of the flow velocity. The positions of the segments were first calculated with the Kirkwood approximation (curves marked "X"), and these positions were then used to calculate the matrix elements in eq 8. Finally the simultaneous equations were solved for the forces on the segments; these are the curves marked "Force" in Figure 9. The Kirkwood force (dot−dash curves) is seen to be a close approximation to the average of the forces from the full solution of eq 8, with the main deviations appearing at the ends of the molecule. The effect of the approximation is thus a minor redistribution of the forces over the molecule, leaving the total force practically the same.

These results suggest that by the use of our eqs A-11 and A-12 for the matrix elements we have avoided the singularities found by Zwanzig and co-workers[13] and that the Kirkwood approximation is unnecessary, but there is still the danger that our algorithm of searching for consistency of forces and positions would be unstable if it were based on the full solutions of eq 8. This question invites future study.

References and Notes

(1) Schwartz, D. C.; Koval, M. *Nature* **1989**, *338*, 520.
(2) Wang, M. D.; Yin, H.; Landick, R.; Gelles, J.; Block, S. M. *Biophys. J.* **1997**, *72*, 1335.

(3) Bustamante, C.; Marko, J. F.; Siggia, E. D.; Smith, S. *Science* **1994**, *265*, 1599.
(4) Smith, S. B.; Finzi, L.; Bustamante, C. *Science* **1992**, *258*, 1122.
(5) (a) Yamakawa, H. *Modern Theory of Polymer Solutions*; Harper and Row: New York, 1971; pp 52−56. (b) Flory, P. J. *Statistical Mechanics of Chain Polymers*; Interscience: New York, 1969; Appendix G.
(6) Perkins, T. T.; Smith, D. E.; Larson, R. G.; Chu, S. *Science* **1995**, *268*, 83.
(7) Kirkwood, J. G. *J. Polymer Sci.* **1954**, *12*, 1. F_{kw} can also be thought of as the first term of a polynomial expansion of the F_j in terms of powers of j. See also the discussion by Yamakawa: eqs 32.41 and 32.42 in ref 5a.
(8) Larson, R. G; Perkins, T. T.; Smith, D. E.; Chu, S. *Phys. Rev. E.* **1997**, *55*, 1794.
(9) Marko, J. F.; Siggia, E. D. *Macromolecules* **1995**, *28*, 8759.
(10) Bustamante, C.; Stigter, D. *Biophys. J.*, in press.
(11) Batchelor, G. K. *J. Fluid Mech.* **1970**, *44* , 419.
(12) Kirkwood, J. G.; Riseman, J. *J. Chem. Phys.* **1948**, *16*, 565. See also a discussion in: Doi, M.; Edwards, S. F. *The Theory of Polymer Dynamics*; Clarendon Press: Oxford, England 1989; p 68. We tried using the more exact matrix of Rotne and Prager (Rotne, J.; Prager, S. *J. Chem. Phys.* **1969**, *50*, 4831) but found that it made almost no difference.
(13) Zwanzig, R.; Kieffer, J.; Weiss, G. H. *Proc. Natl. Acad. Sci. U.S.A.* **1968**, *60*, 381.
(14) Lighthill, J. *SIAM Rev.* **1976**, *18*, 161.
(15) Vologodskii, A. *Macromolecules* **1994**, *27*, 5623.
(16) Consider a long wormlike chain of contour length C stretched by a force oriented along the x-axis, so the mean x-component of the end-to-end distance is X. Let this be conceptually divided into k equal segments each with the same contour length c. It is important to note that the segments are viewed as unmodified parts of the chain; they have not been detached, nor have free joints been introduced between them. Since the segments all have the same properties, and are all subject to the same stretching force, the x-components of their mean end-to-end extensions x are all the same, and must sum to X. Hence $X/C = x/c$, which is to say that the force law is the same for all segments, independent of the value of k or of the initial contour length C. Note, however, that we have assumed that the force applied to the ends is the only force. But in our model the real forces are distributed over all segments, thus assuming that all have the same force law is an approximation.
(17) Perrin, F. *J. Phys. Radium* **1936**, *7* (7), 1, eq 102. This formula comes from the exact solution of the equations for the flow around the ellipsoid. Strictly speaking, it gives the average *mobility* of the randomly oriented ellipsoid; when we use it for the average *resistance*, we are making a small approximation. The basic formulas for the ellipsoid were derived by Oberbeck, A. *J. Reine Angew. Math.* **1876**, *81*, 62.
(18) We used two procedures from: Press, W. H.; Flannery, B. P; Teukolsky, S. A.; Vetterling, W. T. *Numerical Recipes in Pascal*; Cambridge University Press: Cambridge, England, 1989. The root-finding function ZBRENT for the F_{tot} search and the minimum-finding function BRENT for the best-fit value of P. These functions efficiently combine the method of bisecting the interval with inverse quadratic interpolation to find a root or minimum.
(19) Hagerman, P. J. *Annu. Rev. Biophys. Biophys. Chem.* **1988**, *17*, 265.
(20) Reference 9, p 8767, eqs 25 and 27, with eq 5.
(21) Smith, D. E.; Perkins, T. T.; Chu, S. *Macromolecules* **1996**, *29*, 1372.
(22) Long, D.; Viovy, J. L.; Ajdari, A. *Biopolymers* **1996**, *39*, 755.
(23) Cluzel, P.; Lebrun, A.; Heller, C.; Lavery, R.; Viovy, J.-L.; Chatenay, D.; Caron, F. *Science* **1996**, *271*, 792.
(24) Smith, S. B.; Cui, Y.; Bustamante, C. *Science* **1996**, *271*, 795.
(25) Burgers, J. M. *Second Report on Viscosity and Plasticity of the Amsterdam Academy of Sciences*, Nordeman Publishing Company: New York, 1938; Chapter 3.
(26) Oseen, C. W. *Neuere Methoden und Ergebnisse in der Hydrodynamik*; Akademische Verlagsgesellschaft: Leipzig, Germany, 1927.
(27) Hermans, J. J. *Recl. Trav. Chim. Pays-Bas* **1944**, *63*, 219.
(28) Zimm, B. H. *J. Chem. Phys.* **1956**, *24* , 269.
(29) Hancock, C. J. *Proc. R. Soc. London* **1953**, *217*, 96.

MA980643N